LWS: A LoRaWAN Wireless Underground Sensor Network Simulator for Agriculture Applications

Shiyang Wu*, Kevin I-Kai Wang*, Ameer Ivoghlian*, Andrew Austin*, Zoran Salcic*, and Xiaokang Zhou†

*Department of Electrical and Computer Engineering, The University of Auckland, New Zealand
†Faculty of Data Science, Shiga University and RIKEN Center for Advanced Intelligence Project, Japan
Email: swu145@aucklanduni.ac.nz, kevin.wang@auckland.ac.nz

Abstract—Wireless Underground Sensor Networks (WUSNs) is an emerging area of IoT applications. However, the current wireless sensor networks yield results that are not feasible nor scalable for a real-world application due to their short transmission range in an underground environment. The emerging technology of Low Power Wide Area Network (LPWAN) which promises large numbers of devices at long range and low energy consumption offers a potential solution for WUSN applications. Among the existing LPWAN technologies, LoRa/LoRaWAN is one of the most popular choice providing reasonable data rate at long range and low power consumption. This paper focuses specifically on LoRa/LoRaWAN technology as a potential solution for WUSNs in agriculture applications. A novel discrete event LoRaWAN WUSN simulator, *LWS*, is designed to incorporate a soil path loss model, which enables more accurate modelling of WUSNs in a real deployment. The feasibility and scalability of LoRaWAN in WUSN applications are investigated and demonstrated through simulations.

Index Terms—WUSN, LPWAN, LoRa, LoRaWAN, Simulator

I. INTRODUCTION

Wireless Underground Sensor Networks (WUSNs) consists of wireless nodes which are completely buried beneath the surface of the earth and potentially cause less interference to operations above the ground. WUSNs can be highly beneficial to some applications such as agriculture, underground structure monitoring, landscape management and border security. When completely buried, sensor nodes are expected to be very power efficient and able to operate without human intervention for a long period of time [1]. Since the propagation medium includes soil, it is challenging to design a network that is feasible and scalable for underground applications [2].

Taking agriculture applications as an example, typically these do not need high deployment density and fast data rate, but do require larger deployment coverage and long operating life. Previous demonstrations of WUSN deployment with technologies such as Zigbee [3], Mica [4] and magnetic induction waveguides [5], all showed limited transmission range within 10 metres.

The recent development of Low Power Wide Area Network (LPWAN) technologies such as LongRange (LoRa) [6], Sigfox, NB-IOT [7] offer the potential to deploy a WUSN with increased coverage area, better scalability and long operating life. Among the existing LPWAN technologies, LoRaWAN is considered to be one of the most popular due to its open standard, high immunity to interference, AES-128 encrypted packets and long communication range. This paper investigates the challenges and trade-offs of deploying a WUSN using LoRa/LoRaWAN for agriculture applications.

In order to study the feasibility and performance of LoRaWAN in the context of WUSN, a new discrete event simulator based on the works of [8] and [9] is presented. The proposed LoRaWAN WUSN Simulator (LWS) incorporates an underground soil path loss model using the dielectric properties of soil [2] [10] [11]. This allows developers to simulate network deployment more close to the real world scenario. Through simulation, we can easily adjust soil conditions, deployment conditions and network parameters, to study the feasibility and scalability of LoRaWAN for WUSN applications. In this paper, we demonstrate the impact and performance simulations of LoRaWAN with different burial depth, coverage area, and node density, in the context of agriculture applications.

The paper is organised as follows. Section II provides an overview of the related works on WUSNs and the fundamentals of LoRaWAN. Section III describes the soil path loss model we adopted in this research. Section IV presents the LoRa-specific network features/parameters and environmental parameters that are included in LWS. Section V discusses the simulation results that demonstrate the LoRaWAN performance under different deployment conditions. Section VI concludes the paper.

II. RELATED WORKS

A. WUSN

In [2], a propagation model for Electromagnetic (EM) waves in soil was presented using the dielectric properties of soil investigated by [10]. The path loss introduced by soil is much more significant than air due to the moisture content and absorption. Path loss is dependent on soil conditions, e.g. soil composition, volumetric water content (VWC), bulk density and particle density. Path loss is also dependent on the frequency, with lower path loss observed at lower frequencies. In [2], authors used a MICA2 Mote operating at 300 MHz, with a propagation range of 4 metres. This theoretical basis was validated by the test bed developed in [3]. However, both studies [2] [3] focus on the traditional wireless sensor networks with FSK modulation while LoRa uses Chirp Spread Spectrum (CSS) modulation, which is more robust in terms of having a high immunity to interference, making the sensitivity of the receivers as low as -130 dB.

There are also other approaches that make use of magnetic induction (MI) based transmission. The usage of MI transceivers for WUSN has been suggested in [5]. MI transceivers utilise induction coils to generate quasi-static magnetic fields [12] which can be sensed by receiving coil, establishing a communication link between the sending soil and the receiving coil. The structure of MI-based WUSNs presented in [5] consists of multiple underground nodes and a sink node which is connected to the gateway that will upload the data sent by the buried nodes to the cloud for further processing.

In [13], a proof-of-concept WUSN deployment using Sig-Fox, Thoreau, was presented. Thoreau has been deployed in harsh conditions with the underground environment and cold weather, and proved to be a successful prototype even though SigFox is not optimised for underground environments. The maximum range that was achieved in [13] was 1.82 km away from the SigFox base station. The burial depth of sensors ranges from 15 cm to 35.6 cm so that they will not interfere with topsoil activities. The Thoreau network prototype has a total of 8 SigFox end-devices operating at 902 MHz and one SigFox base station to collect data such as soil moisture readings and temperature readings. As a proof of concept, [13] shows great potential for using LPWAN technologies as WUSN deployments.

B. LoRa and LoRaWAN

LoRa and LoRaWAN are emerging LPWAN technologies and promise long-range and low-power transmission. In [14], it was shown that the communication range of LoRa could reach 5 to 10 km in rural areas and up to 30 km above the water (i.e. with line of sight). In addition, [15] shows a case study for deploying LoRaWAN in an indoor environment where a larger amount of attenuation is present. However, the results show that floors of a building do not have significant impact on the packet loss of the network. It was also shown that different LoRa transmission settings would affect the sensitivity and hence the packet loss of the network. These results from real world deployment case studies [14] [15] suggest the feasibility of deploying a LoRaWAN-based WUSN.

In [8], a LoRaWAN simulator, *LoRaSIM*, was proposed. This simulator offers a simulation framework that uses the transmission parameters of a LoRa node and several collision behaviours to estimate the scalability of a LoRaWAN network. Some limitations are present with LoRaSIM as it lacks features that simulate LoRaWAN MAC layer behaviours. In order to study the feasibility and scalability of deploying a LoRaWAN-based WUSN, LoRaSIM needs to be extended to simulate additional LoRaWAN behaviours. In [9], a LoRaWAN simulator, *LoRaWANSIM*, was improved based on *LoRaSIM* with some of the LoRaWAN MAC layer features including downlink possibility, control messages, acknowledgements and retransmission strategies. However, since the focus of [9] does not include the applications of WUSN and its source code is not publicly available, we implemented our LoRaWAN-WUSN simulator with both LoRaWAN MAC layer features

and underground path loss model to provide a realistic simulation for a LoRaWAN-based WUSN.

III. PROPAGATION OF EM WAVES IN SOIL

In order to study the performance of WUSN, it is critical to model the signal propagation and soil path loss to better reflect real world deployment conditions. This section introduces the soil path loss model used and implemented in LWS.

A. Dielectric Properties of Soil

The path loss of an EM wave propagating through a soil medium depends on the dielectric properties. The dielectric properties of soil are defined by parameters including the complex dielectric permittivity, electrical conductivity and magnetic permeability of the soil.

The complex dielectric permittivity of soil describes the ability for the soil to permit the transmission of an electric field [16] and is described by:

$$\epsilon = \epsilon' - j\epsilon'' \tag{1}$$

where ϵ is the complex dielectric permittivity, ϵ' is the real part of complex dielectric permittivity which is related to the storage of energy, ϵ'' is the imaginary part of dielectric permittivity which is related to relaxation and dispersive loses and $j = \sqrt{-1}$. The physical factors that affect the dielectric permittivity are the water content, the frequency of the signal, the soil composition, and the soil conductivity. There are several models to estimate the complex permittivity as it is difficult to measure in-situ. These models [16] are based on parameters that are easy to measure such as water content and the composition of soil. For our research, we chose the Peplinski model [10] to describe the dielectric properties of soil as it is one of the most widely used models that supports different soil types.

The electrical conductivity of soil describes the ability of the soil to conduct electrical currents. This affects the imaginary part of the complex dielectric permittivity of soil [17]. The conductivity of soil can be measured in the laboratory or at the deployment site with a wide range of techniques such as Time Domain Reflectometry [17]. Other than measuring the conductivity on site, the Peplinski model includes a term to account for the effective conductivity of the soil mixture in the imaginary part of the complex dielectric permittivity of soil [10].

The relative magnetic permeability of soil is commonly described using the ratio between the magnetic permeability of soil and free space. For most common soil types, the relative magnetic permeability can be assumed to be 1.0 [18].

B. Path Loss Model

In order to accurately simulate the performance of a WUSN, the attenuation of EM waves propagating underground is required. There are two main models to predict the path loss introduced by the soil. The first is the modified Friis model [2] [11] that considers the path loss introduced by the change in wavelength and the attenuation caused by the soil absorption.

The modified Friis model uses the Peplinski model [10] to estimate the complex permittivity of soil. The second model is a semi-empirical model based on the Complex Refractive Index Model (CRIM) [3] which also considers losses due to reflection when calculating the attenuation. The CRIM model uses a mixing model for estimating the complex permittivity of soil. Both models make use of a link budget formula [1] that appends an additional path loss factor L_s introduced by soil to the well known Friis equation:

$$P_r = P_t + G_r + G_t - L_0 - L_s \tag{2}$$

where L_0 is the path loss in free space in dB [19], G_r and G_t are antenna gains in dBi for receiver and transmitter and P_r and P_t are receiver and transmitter powers in dBm respectively.

In [20], an extensive field measurement was conducted in order to compare the accuracy of the modified Friis model [2] [11] and the CRIM-Fresnel model [3] at different field locations with different soil types. It was demonstrated that the calculations based on the modified Friis model more closely fits field measurements than the results of the CRIM-Fresnel model. Therefore, in this paper, the modified Friis model is used to calculate the attenuation introduced by soil.

The modified Friis model presented in [2] [11] considers both attenuation caused by the absorption of EM waves in the soil and the change in wavelength. Based on the modified Friis model, the path loss of EM waves propagating through soil, L_s is given by:

$$L_s = L_\alpha + L_\beta \tag{3a}$$
$$L_\alpha = 8.69\alpha d \tag{3b}$$
$$L_\beta = 154 - 20\log(f) + 20\log(\beta) \tag{3c}$$

where d is the distance between the transmitter and receiver, f is the operating frequency, α and β are attenuation constant and phasing shifting constant described by the Peplinski model [10]:

$$\alpha = \omega\sqrt{\frac{\mu\epsilon'}{2}\left[\sqrt{1 + \left(\frac{\epsilon''}{\epsilon'}\right)^2} - 1\right]} \tag{4a}$$

$$\beta = \omega\sqrt{\frac{\mu\epsilon'}{2}\left[\sqrt{1 + \left(\frac{\epsilon''}{\epsilon'}\right)^2} + 1\right]} \tag{4b}$$

where $\omega = 2\pi f$ is the angular frequency, μ is the magnetic permeability and the real and imaginary part of dielectric permittivity (ϵ' and ϵ'') are estimated by using the Peplinski model [10].

Using the modified Friis model, the path loss at different frequencies, moisture levels and soil conditions can be calculated. Fig. 1 shows the computed path loss values (in dB) at the burial depth of 1 m with soil composition of 50% sand and 10% clay. As the volumetric water content (VWC) is the indication of moisture level of soil content, it is one of the key factors that affects the path loss in the Peplinski model. Fig. 1 shows different VWC levels from 5% to 35% to demonstrate the effect of VWC with increasing path loss.
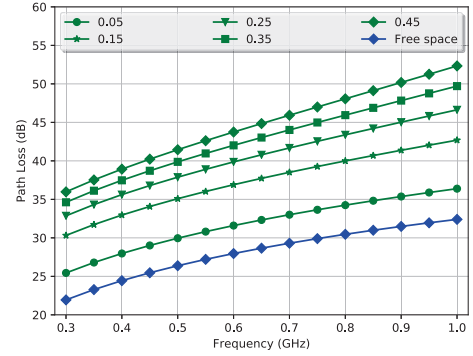

Fig. 1: Path Loss Results with Different Frequencies at Different VWC Levels

IV. SIMULATION

The purpose of conducting simulations is to gather a theoretical guideline for WUSN design before the actual deployment process. In this section, the fundamentals of LoRa and LoRaWAN (or more specifically, the network parameters that exhibit significant impact to a LoRaWAN network) are introduced together with the LWS. Several simulations are conducted to explore the performance and scalability of a LoRaWAN network with multiple underground nodes and a single overground gateway.

A. Overview of LoRa and LoRaWAN

LoRa [6] is the physical layer of LoRaWAN [21]. LoRa employs Chirp Spread Spectrum (CSS) modulation for long range, low power and low data rate wireless transmissions. LoRaWAN is the MAC layer protocol that consists of three network entities: end-devices, gateways and a central network server. End-devices only communicate with a single or multiple gateways via LoRa radio transmissions. Gateways can then communicate with the central network server via IP protocol. This forms a star topology as shown in Fig.2.
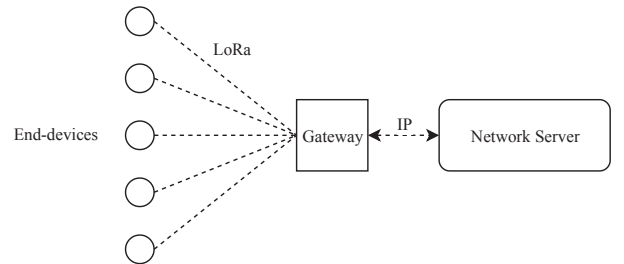

Fig. 2: A typical LoRaWAN network topology

LoRaWAN introduces three classes of operation. Class A is the default and the most supported class, whereas Class B and C are optional classes. Class A defines the operational mode that is required for all LoRaWAN devices and focuses mainly on the uplink traffic (i.e. end-devices to gateway). Therefore, Class A is the most power-efficient out of all three classes

due to its substantial "downtimes" between transmissions, which also results in the lowest data rate among all the operation modes. Class B and C improve on the number of downlinks from the gateways with the price of reduced power-efficiency and not all end-devices support these operation modes. Therefore, for a WUSN application that requires little to no human intervention, Class A is considered the most suitable operation mode to ensure long operating life of end-devices.

There are three transmission parameters in the LoRa PHY layer that can be configured to balance between range, data-rate and energy consumption:

a) Spreading Factor (SF): LoRa technology adopts a spread spectrum modulation scheme that uses wideband linear frequency modulated pulses whose frequency increases or decreases over a certain amount of time to encode information. Therefore, with the spread spectrum, each bit of information is encoded as multiple chips. Each frame is transmitted with a specific SF which can be defined as $SF = log_2(R_c/R_s)$ where R_c is the chip rate and R_s is the symbol rate. The SF describes how many bits per symbol are encoded [6]. The SF ranges from SF7 (128 chips/symbol) to SF12 (4096 chips/symbol) [22]. A higher SF increases the signal to noise ratio (SNR) and hence improves the transmission range due to higher sensitivity of the transceiver. On the other hand, this also results in a slower data rate and longer time on air. Notably, different SF configurations are orthogonal which means that transmissions with different SF values will not collide with each other.

b) Bandwidth (BW): Bandwidth is the range of frequencies in the transmission band. High bandwidth will result in a higher data rate and thus shorter time on air, but a lower sensitivity due to the introduction of extra noise and vice versa. Notably, with the modulation scheme of LoRa, data is sent out at a chip rate equal to the bandwidth. A bandwidth of 125 kHz corresponds to a chip rate of 125 kcps.

c) Coding Rate (CR): Coding rate is used by LoRa transceivers to protect against interference. The coding rate can be set to either 4/5, 4/6, 4/7 or 4/8. A higher CR offers more protection, but it will increase time on air. Notably, transceivers with different CR can still communicate with each other if explicit header mode is used as the information of CR is stored in the header of the packet.

In addition to the aforementioned parameters, the duty cycle restriction discussed in [9] [23] is also a critical factor that restricts the scalability of a LoRaWAN network. As configurations of different SF, BW and CR affect the *time on air*, T_{air}, of a packet, the *off time*, T_{off}, will also change as the consequence of the duty cycle restriction. A duty cycle of 1% (e.g. in Europe and North America) [24] can impose a significant restriction on the overall data throughput of a LoRaWAN network. To demonstrate the effect of the duty cycle, T_{off} can be calculated by:

$$T_{off} = \frac{T_{air}}{DutyCycle} - T_{air} \qquad (5)$$

An end-device cannot immediately retransmit its next packet until after T_{off} seconds. If a packet has a T_{air} of 0.2s, then T_{off} will be calculated as 19.8s which means this sub-band will be unavailable for all devices in the sub-band for that duration. The effect of T_{off} period only applies to that particular sub-band and LoRaWAN specification suggests an end-device can switch its transmit channel before each transmission. However, this will have negative impact on the scalability of a LoRaWAN network if increasing number of end-devices are not permitted to transmit in their corresponding sub-bands and try to switch to another sub-band frequently.
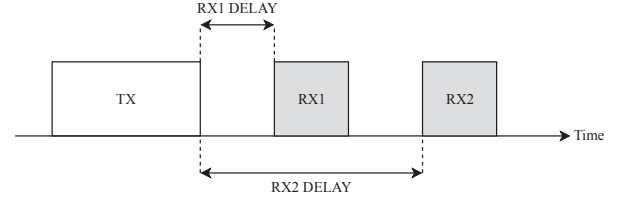

Fig. 3: LoRaWAN Class A Transmission and Reception Slots

The impact of duty cycle and the scalability of a LoRaWAN network becomes even more important when an application requires a node to receive an acknowledgement (ACK) reply from the gateway. Fig.3 shows an example of timing slots for a LoRaWAN Class A end-device where TX slot is used for the uplink data from an end-device to a gateway, and RX1 and RX2 slots are used for receiving downlink data from a gateway. RX slots can be used to carry ACK replies from the gateway. RX1 uses the same frequency channel as the transmission while RX2's channel and data rate can be negotiated between the end-device and gateway. `RX1_DELAY` and `RX2_DELAY` are region specific, for New Zealand and most regions they are set to 1s and 2s. As the duty cycle restriction also applies to the gateway transmitting in a sub-band, when the number of end-devices is large, the gateway may not be able to send an ACK reply in time to some end-devices. This will result in retransmissions from those end-devices if ACK is configured and expected.

B. Simulator Features

On top of the refactored codebase of LoRaSim, features of LoRaWAN are implemented according to the LoRaWAN specification [25]. First, the modified Friis model introduced in Sec. III was incorporated to account for the attenuation of the soil environment in LWS. Also, the transmission parameters were modified according to local (New Zealand) LoRaWAN regulations [24], with centre frequency ranging from 915 to 928 MHz, SF ranging from 7 to 10 and bandwidth of 125 kHz for uplink data and 500 kHz for downlink data.

Currently, LWS offers three performance evaluation metrics, namely the Data Extraction Rate (DER), packet loss and packet collision. The DER is an indication of the overall throughput for a network, therefore retransmitted packets will not count as received packets which can be calculated by:

$$DER = (N_{sent} - N_{lost})/N_{sent} \qquad (6)$$

where N_{sent} is the total amount of packet sent by the end-devices and N_{lost} is the amount of packets lost which includes the collided packets and packets that did not receive an acknowledgement from the gateway. Packet loss is introduced by packets that have been attenuated by the medium so much that the received signal strength is lower than the receiver's sensitivity. Packet collision is a result of various collision behaviours such as frequency collision, timing collision and power collision described in [8].

C. Simulation Process

Sand	Clay	Particle Density	Bulk Density	Gateway Height
40%	40%	1.5g/cm^3	2.66g/cm^3	3m

TABLE I: Fixed Parameters of Simulations

Table I shows the fixed parameters for the conducted simulations in this paper. These parameters are mainly soil properties including the soil composition (sand/clay proportions), particle density, and bulk density. The gateway is configured to be 3 meters above the ground. The values of these parameters are chosen to represent a common top soil composition [2].

VWC	Burial Depth	Deployment Radius	ACK%	Num. Of Nodes
5%	0.1m	10m	5%	30

TABLE II: Default Value for Simulation Variables

Table II shows the variables for each conducted simulation. Each variables will be changed according to the simulation scenario. Table II shows the default value of variables when they are not changing. VWC is the volumetric water content of soil, burial depth is how deep each node (i.e. end-devices) will be buried, deployment radius is the maximum range between a node and gateway, ACK% is the percentage of total nodes that require ACK reply from the gateway according to LoRaWAN MAC specification and Num. of Nodes is all the nodes that will be generated for a simulation.

During each simulation, a number of nodes will transmit packets to the gateway with random starting transmission time every 10 minutes. The total simulation time is 24 hours.

Fig. 4 illustrates the flowchart of the LWS simulation process. The simulation starts by reading the configuration file and pass the parsed arguments to generate the locations for gateway and end-devices with the default burial depth for end-devices. During the simulation process, each end-device will transmit a packet randomly within the set average transmit interval. Transmitted packets will go through several processes of checking. First, the packet will be checked using the path loss model to determine whether the packet will be lost at the receiver side due to signal attenuation. If the packet has reached the gateway successfully, it will be checked for collisions. If the packet requires acknowledgement from the gateway, given that packet encountered no collision, the gateway will attempt to send a downlink acknowledgement packet. If the packet is not acknowledged, the end-device will use the predefined retransmission strategy. If the maximum
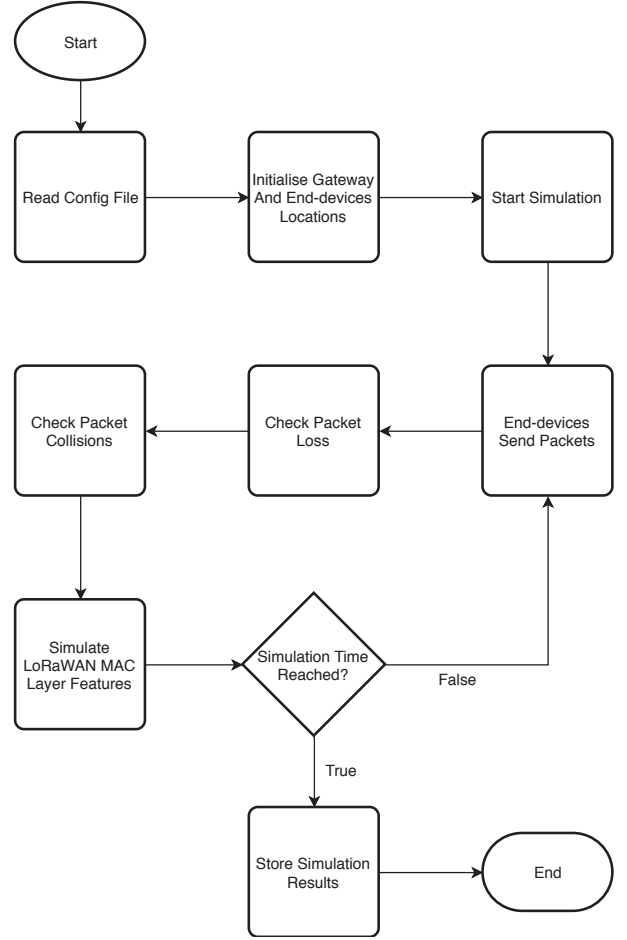

Fig. 4: Simulation Process Flowchart

amount of retransmissions has been reached and still no acknowledgement from the gateway has been received, this packet will be marked as lost as well otherwise the packet has been sent successfully.
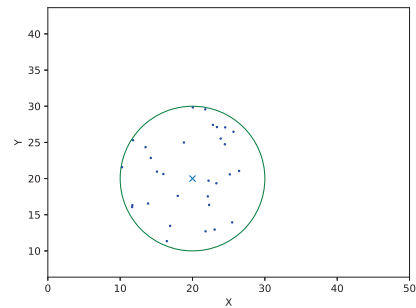

Fig. 5: Randomly Generated Sensor Deployment Positions

At the start of the simulation, positions for each node are randomly generated within the deployment radius as shown in Fig. 5 where the circle indicates the maximum deployment radius, the cross in the centre of circle indicates the position

of the gateway and the scattered dots are randomly generated positions for LoRa-based sensor nodes (i.e. end-devices).
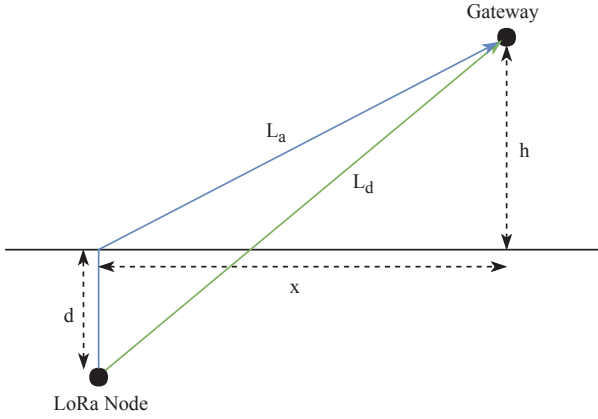

Fig. 6: Two different paths between node and gateway

After a node sends a packet to the gateway, the packet will be assessed with collision criteria in [8] incorporated in LWS. To determine the packet loss of the network, the additional path loss introduced by the soil must be considered. Fig. 6 shows two different propagation paths between the buried node and the gateway where L_d, the green path, is the direct path, L_a, the blue path, is the approximated path which originates from a LoRa node to the ground surface perpendicularly and then follows the free space path between the surface point and the gateway, d is the burial depth of the LoRa node, h is the height where the gateway is placed, and x is the projected distance between the LoRa node and gateway. L_a is the result of refraction between soil and air due to the difference in mediums [26]. L_a and L_d and be calculated by:

$$L_a = d + \sqrt{x^2 + h^2} \tag{7a}$$
$$L_d = \sqrt{(h+d)^2 + x^2} \tag{7b}$$

The approximated path L_a was used to determine the distance between the LoRa node and the gateway considering refraction. Considering the deployment scenario is in a rural area targeting agricultural applications, the path loss model for the above ground part of L_a is selected to be free space [19].

V. SIMULATION RESULTS

By combining the additional path loss introduced by soil, LWS can show the performance of a WUSN in different deployment conditions (e.g. VWC, burial depth and coverage area). For applications that require an ACK reply from the gateway, LWS implements feature in the LoRaWAN MAC layer in order to simulate the behaviour when downlink traffic is required for end-devices.

Simulation variables presented in Table II will be used in pairs to compare their impact on the overall throughput of the network. The pairs of variables are VWC and burial depth, ACK% and the number of nodes, burial depth and deployment radius. The results are plotted against the DER defined in (6) to examine the throughput.
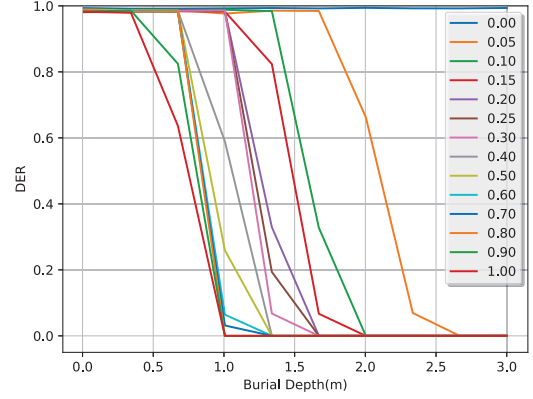

Fig. 7: Burial Depth and VWC Simulation Result

a) Impact of VWC and Burial Depth: Fig. 7 shows the simulation results of comparing the effect of different burial depths ranging from 0 to 3m and VWC values ranging from 0 to 100%. The VWC values have a smaller step of 5% between 0 and 30% and a larger step of 10% between 30% and 100% in order to examine the effect of VWC in detail at lower VWC values. Note that as the modified Friis model can not be computed when VWC is 0 [2], the path loss is calculated with only the freespace model. Fig. 7 shows the range of acceptable burial depths and VWC levels. For a burial depths lower than 50 cm, most VWC levels can sustain a DER > 80% with the exception of extremely moisture soil, i.e. VWC ≈ 100%. Even with deeper burial depth, the network can sustain a DER > 80% with lower VWC levels, i.e. 1.5 m burial is achievable with a VWC < 15%. Fig. 7 also revealed that the burial depth can be as deep as ∼ 1.5 m if the soil is relatively dry, i.e. VWC < 10%.
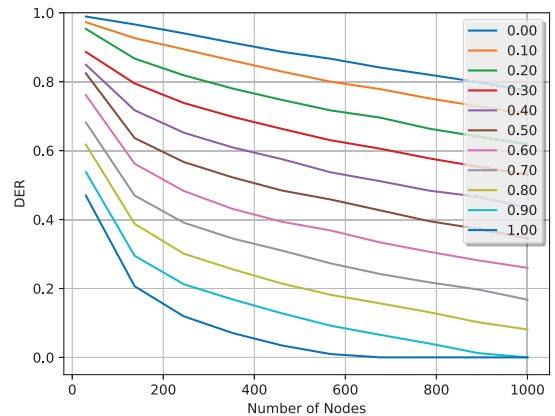

Fig. 8: Results of ACK Percentage and Number of Nodes

b) Impact of ACK Percentage and Number of Nodes Deployed: Fig. 8 shows the simulation results of comparing

the effect of ACK percentage from 0 to 100% at 10% intervals and the number of nodes deployed from 30 to 1000 nodes. The ACK percentage represents the percentage of end devices that requires an ACK reply from the gateway. Lines with different colours shows simulation using a different percentage of nodes that require ACK from the gateway. The duty cycle is set to 1% in this simulation. It is observed that ACK percentage has more significant impact on the DER (i.e. the overall network throughput) than the number of deployed nodes. For increasing amount of nodes that require ACK reply, the duty cycle will quickly become the limiting factor that prevents the gateway from sending an ACK message in time [9] [23]. Without receiving the ACK reply, nodes will have to retransmit the old packet instead of a new packet, therefore, reducing the overall DER.
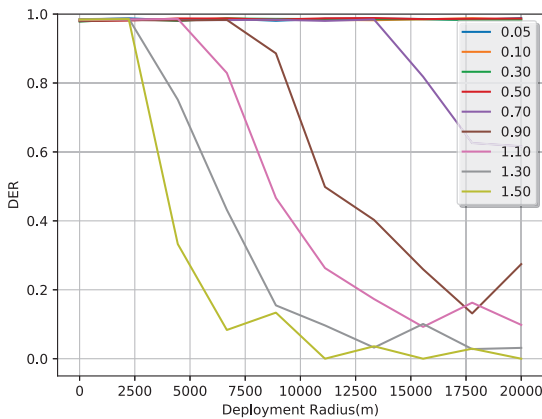

Fig. 9: Results of Burial Depth and Deployment Radius

c) Impact of Burial Depth and Deployment Radius: Fig. 9 compares the effect of changing burial depth from 0.05 m to 1.50 m and deployment radius from 3 m to 20 km. Fig. 9 highlights that in simulation a LoRaWAN WUSN network can still achieve multi-kilometre range of network coverage. With the maximum burial depth of 1.5 m, the network coverage of 2500 m can still be maintained. With a burial depth lower than 70 cm, a network coverage of 20 km can be maintained.

Overall, the simulation results show that all simulation variables affect the DER. In order to provide a reliable communication, a DER of 0.8 or above is required. Considering typical agriculture applications, a burial depth of 0.5 m, deployment radius of 10 km, and ACK rate of 10% are needed. In such deployment scenario, a LoRaWAN WUSN with a single gateway can sustain up to 100% VWC and more than 500 end-devices, which demonstrates good potential for the targeted applications.

VI. Conclusion

In this paper, we presented LWS, a discreet event simulator for LoRaWAN based WUSN. LWS followed and incorporated the LoRaWAN specification and is designed for exploring the feasibility and scalability of LoRaWAN being deployed as a WUSN. By using LWS, real world aspects of deploying a WUSN (i.e. the soil attenuation and path loss) can be taken into consideration prior to the actual system deployment. Existing research showed that there are limitations in LoRaWAN scalability due to duty cycle restrictions. For an agriculture application, as it does not require large deployment density, a LoRaWAN based WUSN may be feasible. Our simulation results show that LoRaWAN can achieve multi-kilometre range of network coverage with a burial-depth within the topsoil region, i.e. less than 70 cm. Additionally, VWC can greatly affect the attenuation level of the signal which will affect the overall DER of the network. Furthermore, the ACK rate of the network can cause network congestion with the regional duty cycle restrictions.

The LWS is a versatile tool for LoRaWAN based WUSN pre-deployment analysis. However, since LoRaWAN uses LoRa as its physical layer, the path loss model may need fine tuning towards the CSS modulation scheme of LoRa to yield a more accurate result. A more accurate path loss model can be obtained by refining our current model with site measurements, which will be conducted in the next step of our research.

References

[1] I. F. Akyildiz and E. P. Stuntebeck, "Wireless underground sensor networks: Research challenges," *Ad Hoc Networks*, vol. 4, no. 6, pp. 669–686, nov 2006.

[2] M. C. Vuran and A. R. Silva, "Communication through soil in wireless underground sensor networks–theory and practice," in *Sensor Networks*. Springer, 2010, pp. 309–347.

[3] Bogena, Heye, J. Huisman, H. Meier, U. Rosenbaum, and A. Weuthen, "Hybrid Wireless Underground Sensor Networks: Quantification of Signal Attenuation in Soil," *Vadose Zone Journal*, vol. 8, pp. 755–761, 2009.

[4] X. Dong, M. C. Vuran, and S. Irmak, "Autonomous precision agriculture through integration of wireless underground sensor networks with center pivot irrigation systems," *Ad Hoc Networks*, vol. 11, no. 7, pp. 1975–1987, sep 2013. [Online]. Available: https://www-sciencedirect-com.ezproxy.auckland.ac.nz/science/article/pii/S1570870512001291

[5] Z. Sun and I. F. Akyildiz, "Magnetic Induction Communications for Wireless Underground Sensor Networks," *IEEE Transactions on Antennas and Propagation*, vol. 58, no. 7, pp. 2426–2435, jul 2010.

[6] "LoRa Modem Designer's Guide," 2013.

[7] U. Raza, P. Kulkarni, and M. Sooriyabandara, "Low Power Wide Area Networks: An Overview," *IEEE Communications Surveys Tutorials*, vol. 19, no. 2, pp. 855–873, 2017.

[8] M. C. Bor, U. Roedig, T. Voigt, and J. M. Alonso, "Do LoRa Low-Power Wide-Area Networks Scale?" in *Proceedings of the 19th ACM International Conference on Modeling, Analysis and Simulation of Wireless and Mobile Systems*, ser. MSWiM '16. New York, NY, USA: ACM, 2016, pp. 59–67. [Online]. Available: http://doi.acm.org/10.1145/2988287.2989163

[9] A.-I. Pop, U. Raza, P. Kulkarni, and M. Sooriyabandara, "Does Bidirectional Traffic Do More Harm Than Good in LoRaWAN Based LPWAN Networks?" *CoRR*, vol. abs/1704.0, 2017. [Online]. Available: http://arxiv.org/abs/1704.04174

[10] N. R. Peplinski, F. T. Ulaby, and M. C. Dobson, "Dielectric properties of soils in the 0.3-1.3-GHz range," *IEEE Transactions on Geoscience and Remote Sensing*, vol. 33, no. 3, pp. 803–807, may 1995.

[11] L. Li, M. C. Vuran, and I. F. Akyildiz, "Characteristics of Underground Channel for Wireless Underground Sensor Networks," 2007.

[12] S. Kisseleff, I. F. Akyildiz, and W. H. Gerstacker, "Survey on Advances in Magnetic Induction based Wireless Underground Sensor Networks," *IEEE Internet of Things Journal*, vol. PP, no. c, p. 1, 2018.

[13] X. Zhang, A. Andreyev, C. Zumpf, M. C. Negri, S. Guha, and M. Ghosh, "Thoreau: A subterranean wireless sensing network for agriculture and the environment," in *2017 IEEE Conference on Computer Communications Workshops (INFOCOM WKSHPS)*, may 2017, pp. 78–84.

[14] J. Petajajarvi, K. Mikhaylov, A. Roivainen, T. Hanninen, and M. Pettissalo, "On the coverage of LPWANs: range evaluation and channel attenuation model for LoRa technology," in *2015 14th International Conference on ITS Telecommunications (ITST)*, dec 2015, pp. 55–59.

[15] P. Neumann, J. Montavont, and T. Noël, "Indoor deployment of low-power wide area networks (LPWAN): A LoRaWAN case study," in *2016 IEEE 12th International Conference on Wireless and Mobile Computing, Networking and Communications (WiMob)*, oct 2016, pp. 1–8.

[16] J. M. H. H. van Dam Brian Borchers, "Methods for prediction of soil dielectric properties: a review," pp. 5794 – 5794 – 10, 2005. [Online]. Available: https://doi.org/10.1117/12.602868

[17] D. A. Robinson, S. B. Jones, J. M. Wraith, D. Or, and S. P. Friedman, "A Review of Advances in Dielectric and Electrical Conductivity Measurement in Soils Using Time Domain Reflectometry," *Vadose Zone Journal*, vol. 2, no. 4, p. 444, 2003. [Online]. Available: http://dx.doi.org/10.2113/2.4.444

[18] N. Chaamwe, W. Liu, and H. Jiang, "Wave propagation communication models for Wireless Underground Sensor Networks," in *2010 IEEE 12th International Conference on Communication Technology*, nov 2010, pp. 9–12.

[19] T. Rappaport, *Wireless Communications: Principles and Practice*, 2nd ed. Upper Saddle River, NJ, USA: Prentice Hall PTR, 2001.

[20] A. M. Sadeghioon, D. N. Chapman, N. Metje, and C. J. Anthony, "A New Approach to Estimating the Path Loss in Underground Wireless Sensor Networks," *Journal of Sensor and Actuator Networks*, vol. 6, no. 3, p. 18, aug 2017.

[21] N. Sornin and A. Yegin, "LoRaWAN 1.1 Specification," oct 2017.

[22] Semtech, "Sx1276/77/78/79 Datasheet," 2016.

[23] F. Adelantado, X. Vilajosana, P. Tuset-Peiro, B. Martinez, J. Melia-Segui, and T. Watteyne, "Understanding the Limits of LoRaWAN," *IEEE Communications Magazine*, vol. 55, no. 9, pp. 34–40, 2017.

[24] "LoRaWAN 1.1 Regional Parameters," jan 2018. [Online]. Available: https://www.lora-alliance.org/sites/default/files/2018-04/lorawantm_regional_parameters_v1.1rb_-_final.pdf

[25] "LoRaWAN Specification v1.1 — LoRa Alliance," 2017. [Online]. Available: https://lora-alliance.org/resource-hub/lorawantm-specification-v11

[26] A. Ishimaru, *Electromagnetic Wave Propagation, Radiation, and Scattering: From Fundamentals to Applications*, 2nd ed. Willey, aug 2017. [Online]. Available: https://www.ebook.de/de/product/21080323/akira_ishimaru_electromagnetic_wave_propagation_radiation_and_scattering.html